Virologica Sinica 37 (2022) 48–59

Contents lists available at ScienceDirect

Virologica Sinica

journal homepage: www.keaipublishing.com/en/journals/virologica-sinica
www.virosin.org

Research Article

Nucleolin interacts with the rabbit hemorrhagic disease virus replicase RdRp, nonstructural proteins p16 and p23, playing a role in virus replication

Jie Zhu [a], Qiuhong Miao [a,b], Hongyuan Guo [a], Aoxing Tang [a], Dandan Dong [a], Jingyu Tang [a], Fang Wang [c], Guangzhi Tong [a,*], Guangqing Liu [a,*]

[a] Shanghai Veterinary Research Institute, Chinese Academy of Agricultural Sciences, Shanghai, 200241, China
[b] Laboratory of Virology, Wageningen University and Research, Wageningen, 6708 PB, the Netherlands
[c] Institute of Veterinary Medicine, Jiangsu Academy of Agricultural Sciences, Nanjing, 210014, China

ARTICLE INFO

Keywords:
Rabbit hemorrhagic disease virus (RHDV)
Nucleolin
Virus replication
RNA-dependent RNA polymerase (RdRp)

ABSTRACT

Rabbit hemorrhagic disease virus (RHDV) is a member of the *Caliciviridae* family and cannot be propagated *in vitro*, which has impeded the progress of investigating its replication mechanism. Construction of an RHDV replicon system has recently provided a platform for exploring RHDV replication in host cells. Here, aided by this replicon system and using two-step affinity purification, we purified the RHDV replicase and identified its associated host factors. We identified rabbit nucleolin (NCL) as a physical link, which mediating the interaction between other RNA-dependent RNA polymerase (RdRp)-related host proteins and the viral replicase RdRp. We found that the overexpression or knockdown of NCL significantly increased or severely impaired RHDV replication in RK-13 cells, respectively. NCL was identified to directly interact with RHDV RdRp, p16, and p23. Furthermore, NCL knockdown severely impaired the binding of RdRp to RdRp-related host factors. Collectively, these results indicate that the host protein NCL is essential for RHDV replication and acts as a physical link between viral replicase and host proteins.

1. Introduction

Rabbit hemorrhagic disease virus (RHDV) is the causative agent of rabbit hemorrhagic disease (RHD), which primarily infects the wild and domestic European rabbit (*Orcytolagus cuniculus*) (Meyers et al., 1991b). The lesions caused by the disease are mainly in the liver, spleen, and lungs, causing acute failure with symptoms of dyspnea, disseminated intravascular coagulation, fulminant hepatic failure, and hepatocellular apoptosis (Alonso et al., 1998; Mikami et al., 1999). RHDV mainly distributes and proliferates in the liver, spleen, and lungs (Liu et al., 2015; Neimanis et al., 2018). In 2010, RHDV2, also called RHDV GI.2 (Le Pendu et al., 2017), was detected for the first time in France (Le Gall-Recule et al., 2013), spreading to other countries in Europe, Australia, Africa and America (Abrantes et al., 2013; Mahar et al., 2018; Rouco et al., 2018; Lopes et al., 2019). RHDV is a nonenveloped positive-sense single-stranded RNA virus, which belongs to the family *Caliciviridae*, genus *Lagovirus*. RHDV virions contain the genomic RNA (gRNA) and an additional 2.2 kb of subgenomic RNA (sgRNA), which is collinear with the 3′ end of the gRNA (Meyers et al., 1991a). The gRNA of RHDV consists of a positive-sense single-stranded molecule of 7437 nucleotides with a virus-encoded protein, VPg, which covalently attaches to its 5′ end (Zhu et al., 2015, 2016). The gRNA also contains two slightly overlapping open reading frames (ORFs) of 7 kb (ORF1) and 351 nucleotides (ORF2). ORF1 is translated into a large polyprotein that is cleaved into the major structural protein VP60, the capsid protein, and seven nonstructural proteins: p16, p23, helicase, p29, VPg, protease, and RNA-dependent RNA polymerase (RdRp). RdRp is a replicase of the viral genome, and it is also prone to mutation, which can accelerate the evolution of the virus (Hukowska-Szematowicz, 2020). ORF2 encodes the minor structural protein VP10 (Meyers et al., 1991a; Wirblich et al., 1995; Morales et al., 2004). The sgRNA, which only encodes VP60 and VP10, usually contributes to the production of high levels of products required during intermediate and late stages of infection (Meyers, 2003). Flanking the coding regions of RHDV is a 5′-terminal noncoding region of nine nucleotides and a 3′-terminal noncoding region of 59 nucleotides (Morales et al., 2004). However, the molecular mechanisms responsible for RHDV replication remain poorly understood, mainly due to the lack of a robust cell culture system for propagation of the virus. In 2013, we developed a

* Corresponding author. Shanghai Veterinary Research Institute, Chinese Academy of Agricultural Sciences, Shanghai, 200241, China.
E-mail addresses: gztong@shvri.ac.cn (G. Tong), liugq@shvri.ac.cn (G. Liu).

https://doi.org/10.1016/j.virs.2022.01.004
Received 23 June 2021; Accepted 15 September 2021
Available online 12 January 2022

RHDV replicon system, which has the ability to automatically replicate in rabbit kidney cells (RK-13 cells) (Wang et al., 2013). Construction of this RHDV replicon system has provided a platform for exploring RHDV replication in host cells. In 2017, we successfully constructed mutant RHDV (mRHDV) in RK-13 cells *in vitro*, which has a specific receptor-recognition motif (Arg-Gly-Asp) on the surface of the capsid protein, characterized by two amino-acid substitutions. mRHDV is recognized by the intrinsic membrane receptor (integrin α3β1) of RK-13 cells, by which mRHDV gains entry, replicates, and imparts apparent cytopathic effects (Zhu et al., 2017).

In this study, RHDV replicase and replicase-related host factors were isolated for the first time and its main components were identified. We found that nucleolin (NCL), a multifunctional nucleolar phosphoprotein that played a role in a variety of cell functions, was necessary for RHDV replication because the replication level of RHDV was significantly affected by knocking down the *NCL* gene in cells. Our data showed that NCL was a link between viral replicase and host proteins.

2. Materials and methods

2.1. Plasmids

The pRHDV-luc plasmid, in which the *VP60* and partial *VP10* genes were replaced with the *Fluc* gene, was generated in our previous study (Wang et al., 2013). To generate pRHDV-luc-HA1, pRHDV-luc-HA2, pRHDV-luc-His1, pRHDV-luc-His2, pRHDV-luc-His1/HA1, pRHDV-luc-His1/HA2, pRHDV-luc-His2/HA1, and pRHDV-luc-His2/HA2 plasmids, in which the HA and His tags were inserted in-frame into RdRp, were generated by fusion PCR (Fig. 1A). The lentivirus-based expression plasmids were generated with a pLOV-CMV-GFP vector, which stored in our laboratory, using In-Fusion HD Cloning kits (No.639649, Clontech Laboratories, Inc., California, USA), according to the manufacturer's instructions. The pLOV-CMV-GFP vector was linearized with *Nhe* I and *Not* I. The plasmids, used in mammalian two-hybrid (M2H) assays, were generated with the pACT and pBIND vectors (No.E2440, Promega Corporation, Madison, USA) using In-Fusion HD Cloning kits. The p3×FLAG-CMV-14 vector (No. E7908, Sigma-Aldrich Corporation,

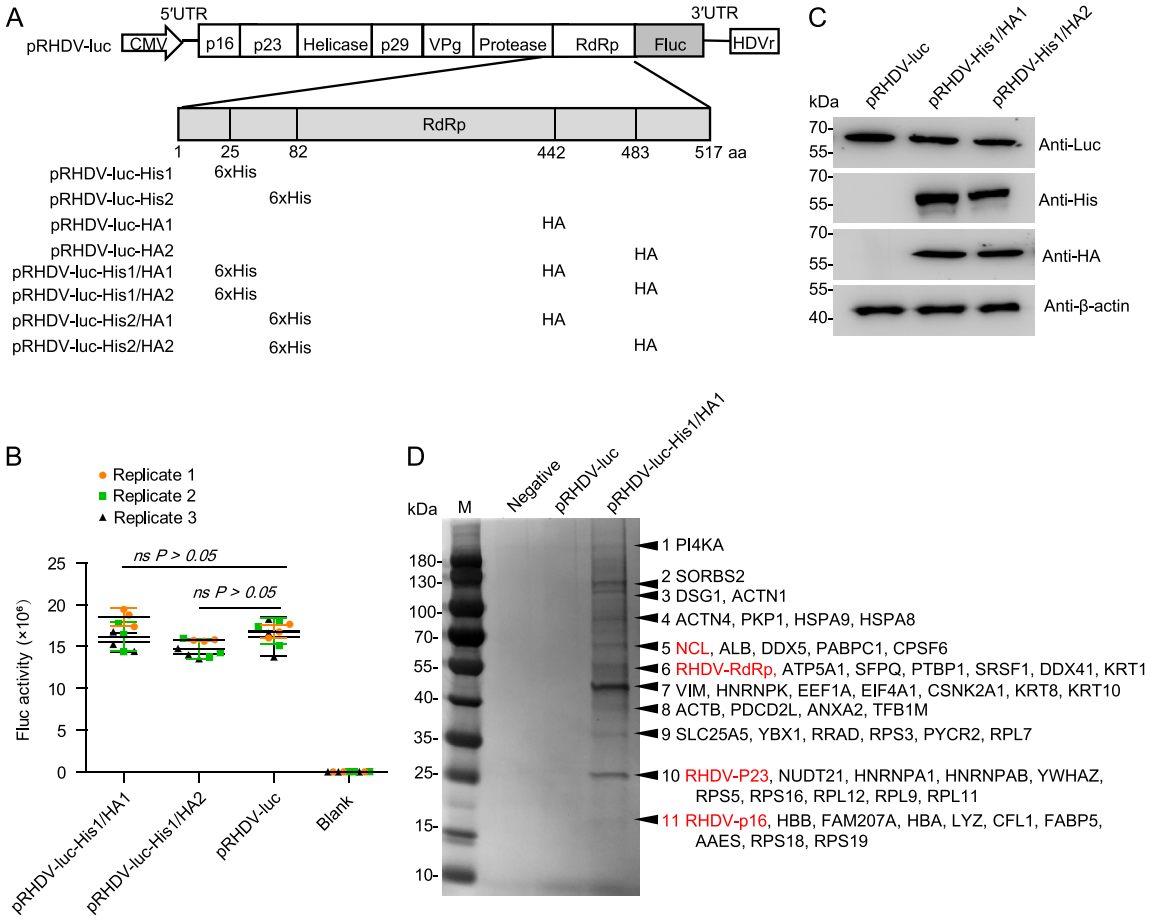

Fig. 1. Affinity purification of solubilized RHDV replicase RdRp-associated host factors. **A** Schematic of RHDV-His/HA replicon constructs. The HA and 6 × His peptide sequences are inserted into the RdRp aa sequence at 25 or 82, 442 or 483 sites, respectively. **B** Effect of the inserted tag on viral replicon activity. RK-13 cells were transfected with recombinant RHDV replicons. Luciferase activity in cell lysates was measured at 48 hpt. Data are shown as mean with SD. Student *t*-tests and analysis of variance were used for statistical analyses. Replicate 1, 2, 3 means three independent experiments, each experiment contains three technical replicate values. The number of cells used in all replicate experiments was similar. **C** Western blotting of recombinant RHDV replicons in RK-13 cells with the antibodies indicated. β-actin was used as an internal control. **D** After two-step affinity purification, the eluted proteins were resolved by SDS-PAGE. Specifically, enriched protein bands (arrows) in the pRHDV-His1/HA1-luc sample were identified by mass spectrometry. Mainly, host proteins and identified viral proteins in the bands indicated are shown. Host factors selected for further study are marked in red. RHDV, rabbit hemorrhagic disease virus; RdRp, RNA-dependent RNA polymerase; hpt, hours post-transfection; SD, standard deviation.

Milwaukee, USA) and pCMV-Myc (No.635689, Clontech Laboratories, Inc.) were used to create mammalian expression constructs. All plasmids were created using In-Fusion HD Cloning kits, according to the manufacturer's instructions. In addition, the primers used in this research are listed in Supplementary Table S1.

2.2. Cell lines and viruses

Rabbit kidney cells RK-13 (ATCC, CCL37) and HEK-293T cells (ATCC, CRL-3216) were routinely maintained in minimal essential medium (MEM) (No. 11090081, Gibco, New York, USA) or Dulbecco's modified Eagle's medium (DMEM) (No.11965092, Gibco), respectively, supplemented with 10% fetal bovine serum (No.04-010-1A, Biological Industries, Beit-Haemek, Israel). RK-NCL cells and RK-GFP cells were generated by transducing RK-13 cells with VSV-G pseudotyped lentiviral particles, which contained the *NCL* gene or *GFP* gene. To generate those recombinant lentiviral particles, we transfected psPAX2 (10 μg), pMD2.G (12 μg), and pLOV-NCL-GFP (22 μg), or pLOV-CMV-GFP (22 μg), respectively, into HEK-293T cells, which were seeded (1×10^6 cells) onto 100-mm tissue culture dishes, using a calcium phosphate transfection reagent (No.K278001, Invitrogen, California, USA). The lentivirus packaging and transduction procedures are based on our previous studies (Zhu et al., 2016). For the RHDV replicon replication assay, these stable cell lines, with exactly the same number of passages, were used to avoid the effect of cell passage variation on RHDV replication.

RHDV strain JX/CHA/97 was isolated in 1997 during an outbreak of RHDV in China and was stored in our laboratory. The genomic sequence of RHDV CHA/JX/97 is available in the GenBank database (accession number DQ205345). mRHDV was mutated from RHDV strain JX/CHA/97 and was stored in our laboratory (Zhu et al., 2017).

2.3. Antibodies and chemicals

The antibodies used in this study included: mouse anti-His (No. ab252883), anti-HA (No. ab18181), anti-luc (No. ab185924), and anti-myc (No. ab32) antibodies purchased from Abcam (Cambridge, England); mouse anti-Flag (No. F3165) obtained from Sigma-Aldrich; mouse anti-β-actin (No. CW0096) and anti-GST (No. CW0084) antibodies purchased from Kangwei Century Biotechnology (Beijing, China); mouse anti-NCL (No. MA1-20800) and rabbit anti-NCL (No. PA5-85973) obtained from Thermo Scientific (New York, USA); mouse anti-RHDV RdRp was prepared by Genscript (Nanjing, China) and was stored in our laboratory; polyclonal rabbit anti-RHDV p16 and anti-RHDV p23 were prepared and was stored in our laboratory; goat anti-mouse IgG conjugated with HRP (No. 123-005-021) and goat anti-rabbit IgG conjugated with HRP (No. 323-005-024) were purchased from Jackson Immuno Research Europe Ltd. (West Grove, USA); goat anti-mouse IgG conjugated with Alexa Fluor 488 (No. A-10680), goat anti-rabbit IgG conjugated with Alexa Fluor 488 (No. A-11008), goat anti-mouse IgG conjugated with Alexa Fluor 633 (No. A-21050), and goat anti-rabbit IgG conjugated with Alexa Fluor 633 (No. A-21070), were obtained from Thermo Fisher Scientific. DAPI staining solution (No. C1002) was purchased from Beyotime Biotechnology (Shanghai, China). *Nhe* I (No. R3131S) and *Not* I (No. R3189S) were obtained from New England Biolabs (Ipswich, USA).

2.4. Affinity purification of host factors associated with RHDV replicase RdRp

RK-13 cells were seeded onto ten 100-mm tissue culture dishes at a density of 1×10^6 cells/dish. The cells were grown overnight and were then transfected with pRHDV-luc-His1/HA1 (12 μg/dish) using Lipofectamine 3000 (No. L3000075, Invitrogen), according to the manufacturer's instructions. After 48 h post-transfection (hpt), the cells were washed for three times with cold Modified Dulbecco's phosphate-buffered saline (No.28344, MDPBS; Pierce™, New York, USA). The cells were then lysed with 500 μL/dish of ice-cold lysis buffer [Tris, 0.15 mol/L NaCl, 0.001 mol/L EDTA, 1% NP-40, 5% glycerol; pH 7.4, proteinase inhibitor cocktail (No.A32955, Thermo Scientific)]. After incubating cells on ice for 5 min with periodic mixing, the lysate was transferred to a microcentrifuge tube and centrifuged at ~ 13,000 × *g* for 10 min to pellet the cell debris. The soluble fraction was incubated by head-to-tail rotation with 300 μL of anti-HA antibody-coated beads (No.88836, Thermo Scientific) for 4 h at 4 °C. The beads were collected by centrifugation and were then washed for four times with 10 mL washing buffer [Tris, 0.15 mol/L NaCl, 0.001 mol/L EDTA, 1% NP-40, 5% glycerol; pH 7.4, 20 mmol/L imidazole (Thermo Scientific)]. After being washed, the bound proteins were eluted with 400 μL of wash buffer supplemented with 250 μg/mL HA peptide (No. I2149, Sigma-Aldrich) by incubation at room temperature (RT) for 10 min. After centrifugation at 3000 × *g* for 5 min, followed by a second elution with 200 μL of wash buffer supplemented with 250 μg/mL HA peptide. The eluted solutions were combined and diluted into 1.5 mL of lysis buffer containing 20 mmol/L imidazole, and 60 μL of Ni Sepharose (No.78606, Thermo Scientific) was added. After incubation at 4 °C for 1 h and clarification, the beads were washed for four times with 1.5 mL wash buffer. The captured proteins were eluted in 80 μL wash buffer containing 240 mmol/L imidazole and were mixed with 20 μL of 5 × SDS loading buffer [250 mmol/L Tris-Cl (pH 6.8), 30% glycerol, 10% SDS, 0.02% bromophenol blue, 25% 2-mercaptoethanol)]. After being boiled for 10 min, the proteins samples were separated by SDS-PAGE, and protein bands were visualized with silver staining.

2.5. Quantitative reverse transcription (qRT)-PCR

Total RNAs were purified using TRIzol reagent (No.15596026, Invitrogen), according to the manufacturer's instructions. DNA was removed from the isolated RNA using DNase I (No.2270A, Takara, Kyoto, Japan), and then cDNA was produced using M-MLV RT (Promega) and random hexamers. The cDNA samples were subjected to real-time PCR with SYBR Premix *Ex Taq* Tli RNase H Plus (No. RR820A, Takara) using an ABI 7500 Fast Real-Time PCR system (Applied Biosystems, USA). The primers are listed in Supplementary Table S1. The relative RNA levels were determined according to the $2^{-\Delta\Delta CT}$ method. The amount of mRNA in each sample was normalized to that of GAPDH.

2.6. M2H assays

The interactions between host protein and RHDV nonstructural proteins were evaluated using a CheckMate Mammalian Two-Hybrid System (No.E2440, Promega). The proteins expressed from the pACT vector recombinant plasmid acted as prey proteins, and proteins expressed from the pBIND vector recombinant plasmid acted as bait proteins. Subsequent M2H analysis was performed, according to the manufacturer's instructions. In brief, bait and prey plasmids were co-transfected with pG5luc plasmids into subconfluent HEK-293T cells at a molar ratio of 1:1:1 for pACT:pBIND:pG5luc vector. At 48 hpt, the HEK-293T cells were lysed, and Renilla luciferase (Rluc) and firefly luciferase (Fluc) activities were evaluated using the Dual-Luciferase Reporter (DLR™) Assay System (No.E1910, Promega).

2.7. Luciferase activity measurements

Cells were washed with PBS and lysed in 200 μL of 1 × Passive Lysis Buffer (No. E194A, Promega). After gentle shaking for 15 min at RT, the cell lysate was transferred to a tube and centrifuged for 2 min at 12,000 × *g* at 4 °C. The supernatant (20 μL) was added to 100 μL of luciferase assay substrate to evaluate the activity of Fluc and Rluc using the Promega DLR™ assay system, based on relative light units (RLUs). Luciferase activity was analyzed using a FB12 luminometer (Berthold, Germany). To normalize the luciferase values determined for cells transfected with the Fluc replicon, Rluc activity was used as an internal control.

2.8. Co-immunoprecipitation (Co-IP) analysis

RK-13 cells were co-transfected with the bait and prey plasmids. At 48 hpt, total protein was isolated from RK-13 cells using IP lysis buffer. We conducted Co-IP analysis using a commercial Co-IP kit (No. 26149, Pierce^{Tm}), according to the manufacturer's instructions. AminoLink Plus Coupling Resin was incubated with anti-myc monoclonal antibody (mAb) (ab32072, Abcam) or anti-Flag mAb (ab205606, Abcam) and then subjected to SDS-PAGE. Immunoblotting (IB) analysis of the proteins was subsequently conducted using mAbs against myc and Flag (Abcam). RNase was added to the cell lysis and wash buffers.

2.9. IB analysis

Protein samples were separated on 12% gels and were then transferred to nitrocellulose membranes (Hybond-C; Amersham Life Sciences, UK) using a semi-dry transfer apparatus (Bio-Rad Laboratories, USA). The membranes were blocked with 5% (w/v) nonfat milk in TBST buffer (150 mmol/L NaCl, 20 mmol/L Tris, and 0.1% Tween-20; pH 7.6) for 3 h at 4 °C and were then stained overnight at 4 °C with a primary antibody (Ab). After washed for three times for 10 min each, the membranes were incubated with a secondary Ab against immunoglobulin G (IgG) conjugated to horseradish peroxidase (No. A0545, Sigma-Aldrich) in PBST buffer (137 mmol/L NaCl, 2.7 mmol/L KCl, 10 mmol/L Na_2HPO_4, 2 mmol/L KH_2PO_4 and 0.1% Tween-20; pH 7.4) for 1 h at RT. Finally, after washed for three times for 10 min each, the proteins were detected using an automatic chemiluminescence imaging analysis system (Tanon Science & Technology Co., Ltd., China).

2.10. Immunofluorescence assay (IFA)

Cells were fixed in 3.7% paraformaldehyde in PBS (pH 7.5) at RT for 30 min and were subsequently permeabilized by incubation in methanol at −20 °C for 30 min. The fixed cells were blocked with 5% (w/v) nonfat milk in PBST buffer for 3 h at 4 °C and were then stained with a primary Ab for 2 h at 37 °C. After washed for three times for 10 min each, the cells were incubated with a secondary Ab against IgG conjugated to fluorescein isothiocyanate (FITC) (No. F0382, Sigma-Aldrich) in PBST buffer for 1 h, at RT. Finally, after washed for three times for 10 min each, the samples were observed under a fluorescence microscope equipped with a video documentation system (ZEISS, Germany).

2.11. Mass spectrometry (MS)

Jingjie PTM BioLab Co., Ltd. (Hangzhou, China) performed all mass spectrometry analyses. The protocol is as follows: first, gel pieces were digested with trypsin at 37 °C overnight. Peptides were extracted with 50% acetonitrile/5% formic acid, followed by 100% acetonitrile. Peptides were dried to completion and resuspended in 2% acetonitrile/0.1% formic acid. Second, the peptides were subjected to nano spray ion (NSI) source followed by tandem mass spectrometry (MS/MS) in Q Exactive™ Plus (Thermo) coupled online to the UPLC. In order to improve the effective of mass spectrometry, the maximum injection time of peptides was set to 20 ms, and the dynamic rejection time of tandem mass spectrometry scanning was set to 15 s to reduce repeated scanning of precursor ions. Automatic gain control (AGC) was set at 5E4. Last, the resulting MS/MS data were processed using Proteome Discoverer 1.3 (Thermo Fisher Scientific Inc, USA). Tandem mass spectra were searched against UniProt *Oryctolagus cuniculus* database (https://www.uniprot.org/taxonomy/9986). Peptide confidence was set at high, and peptide ion score was set >20.

2.12. Statistical analyses

Statistical analysis was performed using GraphPad Prism 6 software. Specific tests are described in the figure legends.

3. Results

3.1. Identification of host factors associated with RHDV replicase RdRp

To discover the host factors that were involved in RHDV replication, we attempted to purify the viral RHDV replicase and replicase-related host factors during viral replication and identify the associated host factors. Previously, the researchers successfully identified hepatitis C virus (HCV) replicase-associated replication complex (RC) components by inserting His and HA tags into the HCV replicon replicase NS5A and NS5B (RdRp) for affinity purification (Yi et al., 2016). Here, we aim to purify RdRp-related host factors by introducing two different tags into RdRp. We generated a recombinant replicon by simultaneously introducing His and HA tag into RdRp (position: 25 or 82 aa for His, 442 or 483 for HA, respectively) of the RHDV replicon (Fig. 1A). Fluc activity and IB analyses showed that RHDV-luc-His1/HA1 and RHDV-luc-His1/HA2 replicated similarly to the untagged RHDV replicon in RK-13 cells ($P > 0.05$, $P > 0.05$, respectively) (Fig. 1B, C). The SWISS-MODEL online tool (https://swissmodel.expasy.org/) predicated that insertion of the His and/or HA tag into these sites does not change the general structure of RdRp, so it is speculated that the insertion into these sites might not significantly affect RdRp activity (Supplementary Fig. S1A). Fluc activity and IB analysis showed that RHDV-luc-His1, RHDV-luc-HA1, and RHDV-luc-HA2 replicated similarly to the untagged RHDV replicon (Supplementary Figs. S1B and S1C). However, the replication level of RHDV-luc-His2 was significantly reduced. We speculate that this site has an important effect on RdRp enzyme activity, and the specific mechanism needs to be further studied.

RK-13 cells were transfected with RHDV-luc-His1/HA1 replicon, which replication level is closest to the untagged replicon, and the cell lysates were sequentially purified using the HA and His tags at 48 hpt. The untagged RHDV replicon acted as a negative control. After two-step affinity purification, the eluted protein complexes were resolved by SDS-PAGE and the protein bands were visualized with silver staining. In total, 11 specific or enriched bands were sliced from the RHDV-luc-His1/HA1 lane and the proteins they contained were identified using MS (Table 1). The identified host proteins were associated with cytoskeleton components, intracellular transport, chaperone, ribonucleoprotein (RNP) components, and translation machine-related proteins. Among these proteins, numerous proteins have been shown to interact with some single-stranded positive-strand RNA viral proteins to regulate viral replication, such as HnRNPK, HSPA8, DDX5, ANXA2, and PI4KA (Hsieh et al., 1998; Saxena et al., 2012; Kovalev and Nagy, 2014; Zhang et al., 2014; Dorobantu et al., 2015) (Fig. 1D and Table 1).

3.2. NCL is involved in RHDV replication

NCL is a phosphoprotein that is ubiquitously and abundantly expressed in many eukaryotic cells and is highly conserved during evolution, as it is involved in a remarkably large number of cellular activities (Jia et al., 2017). It has been confirmed that NCL also plays important roles in the replication and intracellular trafficking of multiple viruses (Tuteja and Tuteja, 1998; Bicknell et al., 2005; Hirano et al., 2005; Becherel et al., 2006;Mongelard and Bouvet, 2007; Abdelmohsen and Gorospe, 2012; Durut and Saez-Vasquez, 2015). To determine if NCL was required for RHDV replication, RK-13 cells were co-transfected with an RHDV replicon, NCL siRNA or Flag-tagged NCL plasmids and internal control plasmid encoding an *Rluc* gene. The reporter luciferase activity was evaluated using a dual-luciferase reporter assay system with cell lysates that were harvested at 24 and 48 hpt. Fluc activity was normalized with respect to a co-transfected plasmid encoding an Rluc. Similar results were obtained in three independent experiments. The results showed that there was a positive correlation between the expression level of Fluc and NCL. The Fluc activity decreased with increasing NCL siRNA transfection dose and increased with increased dose of Flag-NCL transfection (Fig. 2A, B). In previous study, we found that the RHDV replicon

Table 1
Categories of host factors found to be associated with RHDV replicase[a].

Category and band no.	Protein score	Mass (kDa)	Gene name	Protein description	No. of unique peptides	No. of peptides	SC (%)	Category and band no.	Protein score	Mass (kDa)	Gene name	Protein description	No. of unique peptides	No. of peptides	SC (%)
RHDV protein								***Cytoskeleton***							
6	273.3	57.8	*RdRp*	RHDV RdRp	3	4	21.1	11	105.5	14.3	*CFL1*	Cofilin 1	2	6	16.8
10	186.4	25.1	*p23*	RHDV p23	2	3	15.5	3	316.5	102.9	*ACTN1*	Actinin alpha 1	2	7	32.4
11	165.8	16.2	*p16*	RHDV p16	2	4	10.4	4	286.3	87.4	*ACTN4*	Actinin alpha 4	2	6	28.5
Transport								8	357.8	41.7	*ACTB*	Actin, cytoplasmic 1	2	5	19.0
8	57.1	39.2	*ANXA2*	Annexin A2	4	7	10.4	7	419.4	53.6	*VIM*	Vimentin	13	13	25.3
1	201.3	233.6	*PI4KA*	Phosphatidylinositol 4-kinase alpha	6	6	30.5	***Chaperon***							
5	303.5	68.9	*ALB*	Serum albumin	8	10	15.2	7	65.2	45.1	*CSNK2A1*	Casein kinase II subunit alpha	5	5	7.5
11	287.6	15.6	*HBA*	hemoglobin subunit alpha	5	5	40.4	4	236.2	71.0	*HSPA8*	Heat shock cognate 71 kDa protein	7	7	14.2
6	173.2	59.7	*ATP5A1*	F-type H + -transporting ATPase subunit beta	3	3	7.8	9	153.9	30.7	*PYCR2*	Pyrroline-5-carboxylate reductase	4	5	16.8
11	365.6	16.1	*HBB*	Hemoglobin subunit beta	7	9	58.7	3	70.1	116.8	*DSG1*	Desmoglein 1	2	5	9.0
11	365.6	16.1	*HBB*	Hemoglobin subunit beta	7	9	58.7	11	50.3	14.7	*LYZ*	Lysozyme C	2	3	11.5
9	98.3	32.9	*SLC25A5*	Solute carrier family 25	3	3	11.2	4	53.5	73.5	*HSPA9*	Eat shock protein family A (Hsp70) member 9	2	2	13.8
11	99.8	12.6	*FABP5*	Fatty acid-binding protein 5	3	4	13.5	10	152.2	26.2	*NUDT21*	Nudix hydrolase 21	3	3	24.5
RNP complex								8	142.8	40.3	*PDCD2L*	Programmed cell death protein 2-like	4	4	28.7
10	78.5	25.7	*HNRNPA1*	Heterogeneous nuclear ribonucleoprotein A1	3	7	13. 6	11	108.3	16.0	*FAM207A*	Family with sequence similarity 207 member A	5	8	19.6
10	67.9	30.3	*HNRNPAB*	Heterogeneous nuclear ribonucleoprotein A/B	2	6	8.9	***Translation machines***							
7	127.2	50.9	*HNRNPK*	Heterogeneous nuclear ribonucleoprotein K	4	9	11.6	7	94.2	50.0	*EEF1A*	Elongation factor 1-alpha	7	7	9.3
5	87.0	67.5	*DDX5*	DEAD-box helicase 5	2	4	8.3	11	135.4	17.7	*RPS18*	Ribosomal protein S18	4	4	18.7
5	90.6	69.4	*NCL*	Nucleolin	8	10	28.8	11	113.3	16.3	*AAES*	40S ribosomal protein S14	3	3	28.3
2	117.8	130.7	*SORBS2*	Sorbin and SH3 domain containing 2	5	5	14.7	10	174.3	20.2	*RPL11*	Ribosomal protein L11	4	4	20.1
10	135.6	26.2	*NUDT21*	cleavage and polyadenylation specificity factor subunit 5	3	3	10.4	10	283.1	21.2	*RPL12*	Ribosomal protein L12	5	5	33.5
5	99.1	70.9	*PABPC1*	Polyadenylate-binding protein 1	4	4	16.3	11	164.9	12.8	*RPL30*	60S ribosomal protein L30	4	4	50.5
9	128.4	36.0	*YBX1*	Nuclease sensitive element-binding protein 1	5	6	22.1	11	68.3	15.5	*RPS17*	40S ribosomal protein S17	3	3	29.6
6	112.1	57.4	*PTBP1*	Polypyrimidine tract-binding protein 1	4	7	6.7	10	323.2	22.9	*RPS5*	Ribosomal protein S5	7	7	18.5
6	65.2	52.1	*SRSF1*	Splicing factor, arginine/serine-rich 1	6	7	8.8	9	258.2	31.1	*RPS3*	40S ribosomal protein S3	9	9	25.8
5	75.9	63.5	*CPSF6*	Cleavage and polyadenylation specificity factor subunit 6/7	3	10	10.9	7	74.4	45.3	*EIF4A1*	Eukaryotic initiation factor 4A-I	4	6	9.7
6	75.2	62.5	*DDX41*	Probable ATP-dependent RNA helicase	3	12	14.5	11	122.6	13.7	*RPS25*	Ribosomal protein S25	5	5	21.3
								11	75.3	14.0	*RPS15A*	Ribosomal protein S15a	2	5	18.3

[a] Protein lists for each of the proteins identified in Fig. 2B. SC (%) refers to the percent sequence coverage for the protein.

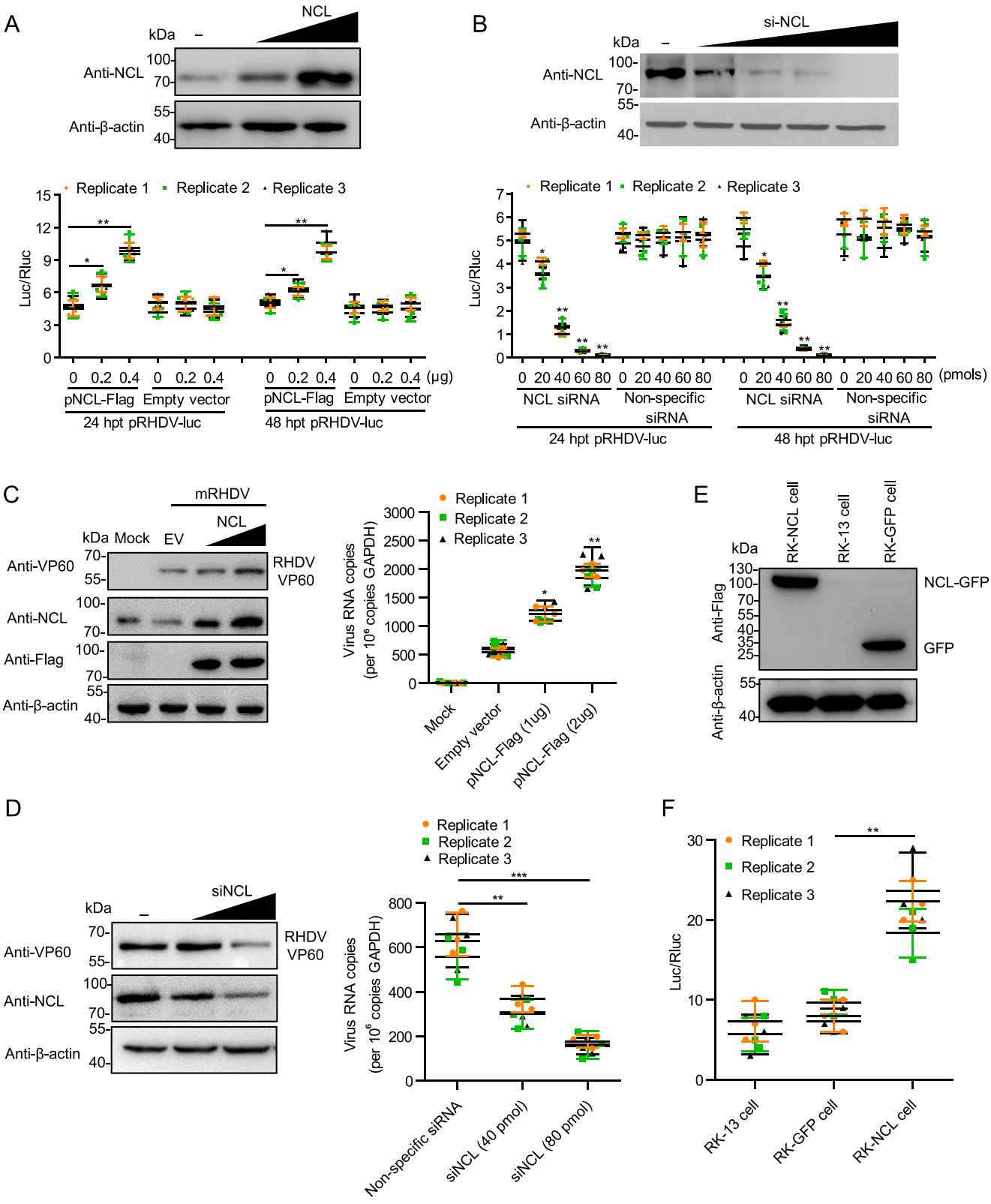

(caption on next page)

activity reached a maximum value at 24 hpt and then declined obviously at 48 hpt (Wang et al., 2013). In this study, it was found that after overexpression of NCL, the replication level of RHDV replicon at 48 hpt was close to the 24 hpt level. Therefore, the expression of NCL promotes RHDV replication in a dose-dependent manner. Subsequently, we examined the effect of NCL on mRHDV, which could proliferate in RK-13 cells (Zhu et al., 2017). We also used NCL siRNA or Flag-tagged NCL to change the expression level of NCL, and then infected the cell with mRHDV (MOI = 1). At 48 h post-infection (hpi), the replication level of mRHDV was detected by Western blotting (WB) and qPCR. The results were similar to RHDV replicons. As shown in Fig. 2C and D, the replication level of mRHDV increased with increased dose of Flag-NCL and decreased with increasing NCL siRNA. In addition, we successfully constructed an RK-NCL cell line, which overexpressed the *NCL* gene, using a lentiviral packaging system (Fig. 2E). To evaluate the replication of RHDV in RK-NCL cells, the cells were co-transfected with an RHDV replicon and internal control plasmid encoding an *Rluc* gene. The reporter luciferase activity was evaluated at 24 hpi. The results showed that the expression level of Fluc in RK-NCL cells was significantly higher than that in control cells (RK-GFP cells and RK-13 cells) (Fig. 2F). Collectively, these data suggest that NCL is involved in RHDV replication.

3.3. NCL interaction with RHDV replicase RdRp, nonstructural proteins p16 and p23

To determine if NCL regulates RHDV replication through interaction with viral nonstructural proteins, we used M2H assays to screen the interaction between NCL and viral nonstructural proteins. As shown in Fig. 3A, NCL interacted with RdRp, p16, and p23. Moreover, an IFA was performed using NCL mAbs, RdRp mAbs, p16 polyclonal antibody and p23 polyclonal antibody in RK-13 cells infected with mRHDV at 24 hpi. As shown in Fig. 3B, NCL was co-localized with RHDV RdRp, p16 and p23 in the RK-13 cell cytoplasm. In addition, the distribution of NCL in the cytoplasm increased after RHDV infection. To determine whether endogenous NCL binds to these viral nonstructural proteins, during RHDV genome replication, we assessed the interaction between NCL and these viral proteins in RK-13 cells, in the presence and absence of mRHDV infection for 24 h at 37 °C. The results of an IP assay performed with cell lysates using NCL mAb showed that regardless of whether the cell lysates were treated with RNase or not, NCL interacted with RdRp, p16, and p23 in infected cells, but did not in uninfected cells (Fig. 3C). To prove NCL interacts with RdRp, p16, and p23, a series of Co-IP assays were used with a myc mAb in RK-13 cells, which were co-transfected with pRdRp-myc, p16-myc, p23-myc and pNCL-Flag eukaryotic expression plasmids. We showed that overexpressed NCL-Flag was present in the anti-myc immunocomplex (Fig. 3D). These results showed that NCL could interact with RHDV RdRp, p16, and p23.

3.4. NCL is a link between RHDV replicase and host proteins

The positive-strand RNA viruses share a conserved replication mechanism in which viral proteins induce host membrane modification to assemble membrane-associated viral replication complex (RCs) (den Boon and Ahlquist, 2010). Viruses hijack host factors to facilitate this energy-unfavorable process (Nagy and Pogany, 2011). Therefore, the components of the viral RC are numerous and complex. NCL is capable of binding to nonstructural proteins (RdRp, p16, and p23) of RHDV. To test the hypothesis that NCL acted as a platform for the RdRp to be attracted to the p16 and p23 proteins, a series of HA tag affinity purification analyses were performed. RHDV-luc-His1/HA1 replicon was co-transfected with NCL siRNA, or non-specific siRNA, in RK-13 cells, respectively, or was transfected in RK-NCL cells. Using IB to detect the purified RdRp-associated protein, we found that the RdRp-associated protein content was significantly reduced in NCL siRNA-treated cells and significantly increased in RK-NCL cells (Fig. 4A). To investigate the specific role of NCL in the formation of RHDV RCs, M2H assays were used to screen the interactions between viral nonstructural proteins and multiple host factors in RCs. As shown in Fig. 4B, there are complex interactions between viral nonstructural proteins and host factors in RCs. For example, p16 interacts with itself, helicase, p29, protease, and NCL; p23 binds to protease and NCL; p29 binds to helicase and VPg; helicase interacts with itself; VPg binds to protease; protease interacts with itself and RPS5; RdRp interacts with RPS5; and NCL binds to HnRNPK, CSNK2A1, RPS5, and RPL11. We subsequently used a series of Co-IP assays with a myc mAb in RK-13 cells, which were co-transfected with bait (myc fusion protein) and prey (Flag fusion protein) eukaryotic expression plasmids. IB analysis using a mAb against Flag showed the specific band corresponding to prey proteins in the myc Co-IP assay (Fig. 4C). These results reveal that RHDV replicase RdRp cannot directly bind to other nonstructural proteins of the virus. It is noteworthy that NCL directly interacts with RHDV RdRp and nonstructural proteins (p16 and p23). Together, these data suggest that RHDV completes its replication process by hijacking NCL to recruit other viral proteins and host factors.

4. Discussion

As an important member of the positive-strand RNA viruses, the *Caliciviridae* family has attracted increasing attention because it contains many viruses that infect a wide spectrum of hosts and are a growing threat to human and animal health. However, most caliciviruses cannot be cultured *in vitro*, including some important pathogens such as RHDV and Norovirus (NV); therefore, the replication and pathogenic mechanisms of these viruses remain poorly understood. The emergence and advancement of reverse genetic manipulation technology has provided an excellent operating platform for revealing the molecular mechanism of calicivirus replication. For example, using a NV replicon, a series of works have been carried out to reveal the mechanism of NV replication (Subba-Reddy et al., 2012; Thackray et al., 2012; Thorne and Goodfellow, 2014; Li et al., 2018; Oliveira et al., 2018). Recently, we also successfully established an RHDV replicon operating platform (Wang et al., 2013) and have applied it to study the genomic structure and function of RHDV.

In this study, we purified viral replicase and identified the replicase-

Fig. 2. NCL is involved in RHDV replication. **A** The effect of NCL eukaryotic plasmids on viral replicon activity. Relative luciferase activity was evaluated in RK-13 cells carrying pRHDV-luc, and *trans*-supplemented NCL eukaryotic plasmids pFlag-NCL (0.2 μg, 0.4 μg) at 24 h post-transfection (hpt) and 48 hpt. The p3 × Flag-CMV-14 vector acted as negative control (−). The luciferase activity in RK-13 cells was evaluated by measuring Fluc activity. Rluc activity was measured to normalize the transfection efficiency. **B** The effect of NCL siRNA on viral replicon activity. The RK-13 cells, co-transfected with pRHDV-luc and NCL siRNA (20 pmol, 40 pmol, 60 pmol, or 80 pmol), were lysed at 24 hpt and 48 hpt, and Fluc activity was measured based on RLUs and normalized according to the results obtained for a co-transfected pLTK plasmid encoding Rluc. The nonspecific siRNA acted as negative control. **C–D** The effect of NCL on mRHDV replication. The RK-13 cells, transfected with pFlag-NCL (1 μg, 2 μg) or NCL siRNA (40 pmol, 80 pmol), were infected with mRHDV (MOI = 1) at 24 hpt, and the level of mRHDV replication were evaluated by Western blotting and qRT-PCR at 48 hpi. The p3×Flag-CMV-14 vector (EV) and nonspecific siRNA (−) acted as negative control. RK-13 cell acted as mock control. **E** The expression level of NCL in RK-NCL cells at 10 passages was determined by Western blotting analysis with anti-Flag mAb. **F** The RHDV replicon replication levels in RK-NCL cells were evaluated by measure Luc at 24 hpi. RK-GFP cells acted as negative controls; RK-13 cells acted as blank controls. Statistical analysis was performed by Student *t*-tests. $^{*}P < 0.05$, $^{**}P < 0.01$ and $^{***}P < 0.001$. Data are shown as mean with SD. Replicate 1, 2, 3 means three independent experiments, each experiment contains three technical replicate values. The number of cells used in all replicate experiments was similar. RHDV, rabbit hemorrhagic disease virus; NCL, nucleolin; hpt, hours post-transfection; SD, standard deviation.

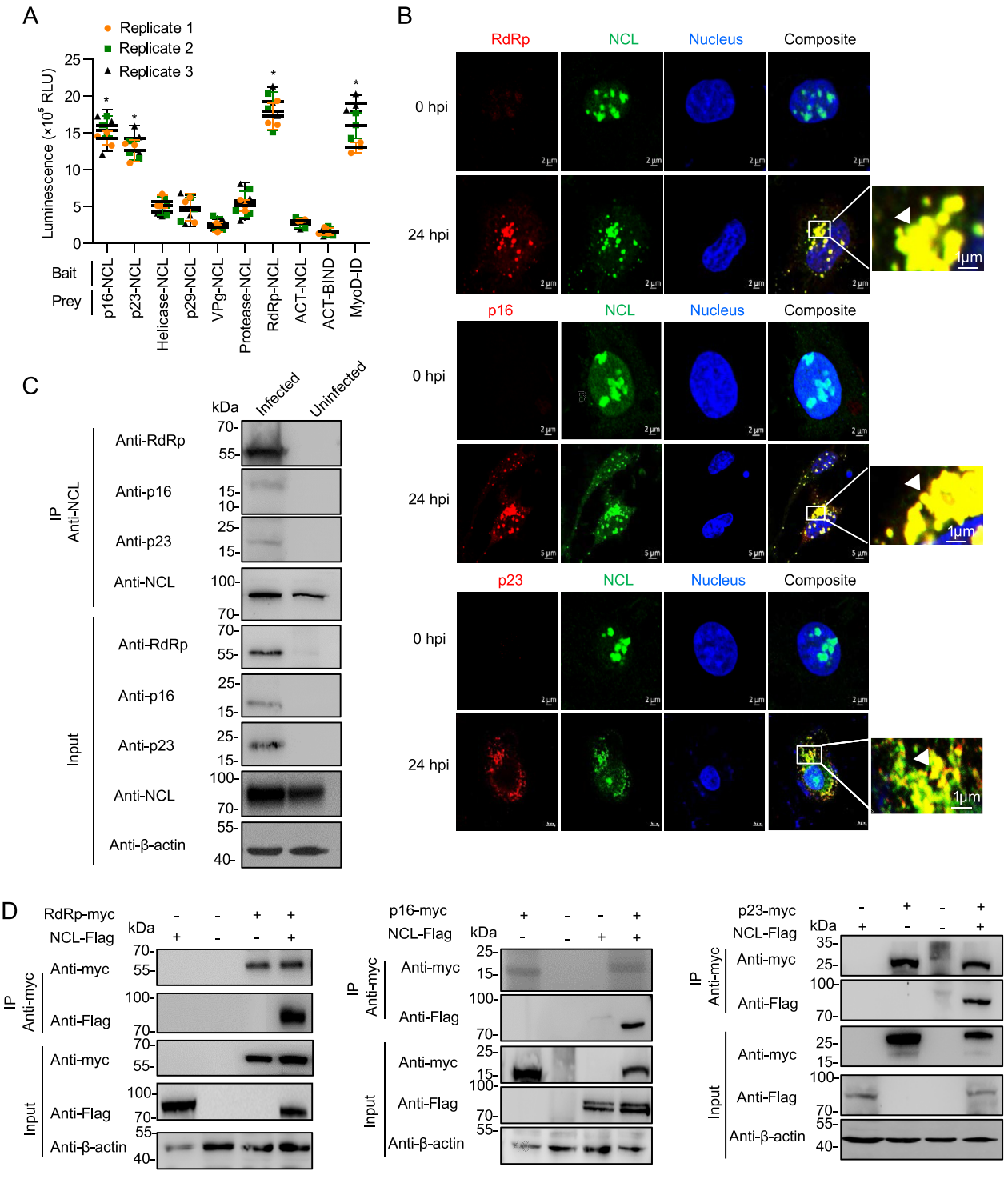

Fig. 3. NCL interacts with RHDV replicase RdRp, nonstructural proteins p16 and p23. **A** M2H interaction of NCL with RHDV nonstructural proteins. Statistical analysis was performed by Student *t*-tests. $^*P < 0.05$. Data are shown as mean with SD. Replicate 1, 2, 3 means three independent experiments, each experiment contains three technical replicate values. The number of cells used in all replicate experiments was similar. **B** Confocal microscopy analysis of NCL (green), RdRp (red), p16 (red) and p23 (red) in RK-13 cells infected with mRHDV at 24 h post-infection with mAbs against NCL and RdRp. The small white boxes represent amplified random co-localization spots within the merged image, and the co-localization spots are indicated with white arrowheads. **C** NCL binds to RdRp, p16 and p23 during RHDV replication. An IP assay was performed on cell lysates using NCL mAb in RK-13 cells that were infected or uninfected with mRHDV, then immunoblotted with Abs against NCL, RdRp, p16 or p23. β-actin was used as an internal control. Cells uninfected with mRHDV served as negative controls. **D** Validation of the interaction of RHDV RdRp, p16 and p23 with NCL in a Co-IP assay. RK-13 cells were co-transfected with the indicated plasmids (+) or empty vectors (−). At 48 h post-transfection, cells were lysed, and IP of myc-fused proteins was performed using anti-myc mAb. Lysates (input) and IPs were analyzed with IB using antibody against myc or Flag. β-actin was used as an internal control. RHDV, rabbit hemorrhagic disease virus; RdRp, RNA-dependent RNA polymerase; SD, standard deviation; NCL, nucleolin; IP, immunoprecipitation; IB, immunoblotting; mAb, monoclonal antibody.

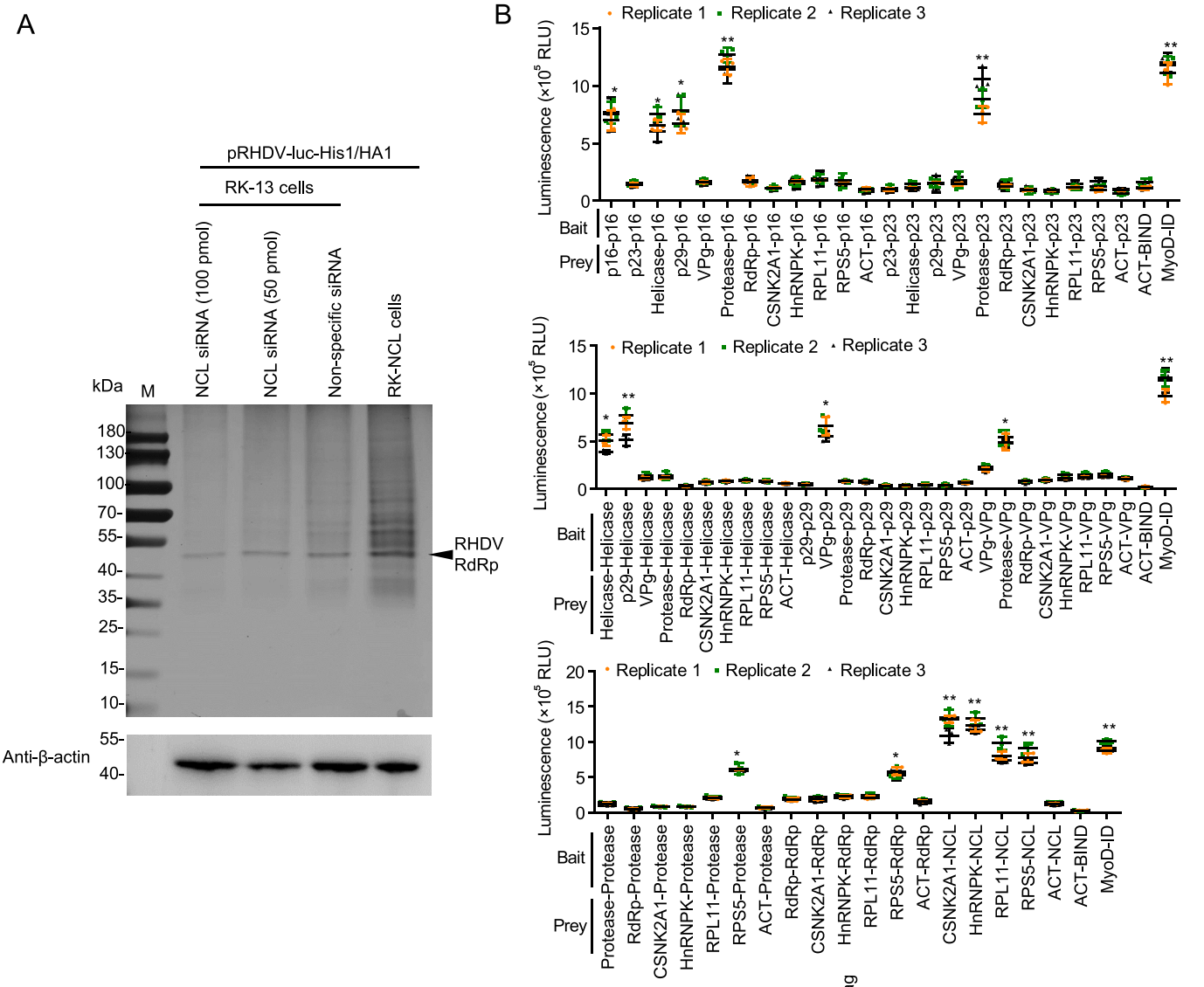

(caption on next page)

Fig. 4. Identification of interactions between RHDV nonstructural proteins and host factors of RCs. **A** NCL siRNA inhibited the formation of the RHDV RC. After HA tag affinity purification, the eluted proteins were resolved by SDS-PAGE. The protein bands were visualized with silver staining. PBS acted as a negative control; β-actin acted as an internal control and was detected by IB with mAb against β-actin. **B** Identification of these interactions by M2H assays. Bait and prey plasmids were co-transfected with pG5luc plasmids into subconfluent HEK-293T cells at a molar ratio of 1:1:1 for the pACT:pBIND:pG5luc vector. At 48 h post-transfection (hpt), the HEK-293T cells were lysed, and Rluc and Fluc activities were evaluated using the Promega Dual-Luciferase Reporter Assay System. All experimental groups were compared with the negative control group (ACT-Bind). Statistical analysis was performed by Student *t*-tests. $^{*}P < 0.05$ and $^{**}P < 0.01$. Data are shown as mean with SD. Replicate 1, 2, 3 means three independent experiments, each experiment contains three technical replicate values. The number of cells used in all replicate experiments was similar. **C** These interactions were verified using Co-IP assays. RK-13 cells were co-transfected with bait and prey plasmids. Cell lysates were prepared 48 hpt and the proteins were subjected to IP followed by IB analysis. myc fusion proteins acted as bait proteins and Flag fusion proteins acted as prey proteins. RHDV, rabbit hemorrhagic disease virus; RC, replication complex; IP, immunoprecipitation; IB, immunoblotting; mAb, monoclonal antibody; SD, standard deviation.

associated host factors using an RHDV replicon system in which two different affinity tags were simultaneously inserted in-frame into RdRp. We determined that NCL played a key role in the formation of RHDV RCs. On the one hand, NCL binds to RHDV replicase (RdRp) (Fig. 3). Similar to other positive-sense RNA viruses, RHDV RdRp has a central role in the viral replication cycle. RdRp has many enzymatic properties; it binds template RNAs, initiates replication, catalyzes elongation, and terminates replication (Urakova et al., 2017b). Moreover, RdRp is able to induce the redistribution of Golgi membranes in kidney and liver cell lines of three different species (Urakova Nadya et al., 2017a). In addition, previous studies have also shown that a certain percentage of RHDV RdRp enters the nucleus, but its role is still unclear (Urakova et al., 2015). On the other hand, NCL also interacts with some important host factors, such as HNRNPK, RPL11, CSNK2A1, and RPS5 (Figs. 1 and 4). Previous studies have shown that these proteins are involved in the replication of various viruses. For example, HNRNPK has been reported to recognize the 5′-terminal sequence of HCV RNA (Fan et al., 2014); CSNK2A1 interaction with NS1 plays an important part in parvovirus replication (Nüesch and Rommelaere, 2006); and RPL11 and RPS5 are components of the ribonucleoprotein complex (Maggi et al., 2008; Robledo et al., 2008). Therefore, we hypothesize that these host factors may also be involved in the replication of RHDV.

We also identified that NCL interacts with nonstructural proteins (p16 and p23) of RHDV (Fig. 3). Previous studies have reported that p16 can accumulate in subnuclear compartments, which may point to a specific interaction with nucleic acids and/or cellular proteins (Urakova et al., 2015). A similar nuclear/subnuclear accumulation of nonstructural proteins has been reported in picornavirus, for which nuclear accumulation of the 2A protein and a close association of this protein with the nucleolar ribosomal chaperone protein B23 have been reported. It was suggested that 2A upregulated the formation of modified ribosomes with a preference for viral internal ribosomal entry sites, thereby contributing to the inhibition of cap-dependent cellular mRNA translation (Aminev et al., 2003). The N-terminal domain of NCL contains acidic regions, rich in glutamic acid and aspartic acid, which are the sites of phosphorylation and participate in the transcription of rRNA and interact with components of the pre-rRNA processing complex (Jia et al., 2017). Therefore, we speculate that RHDV utilizes the interaction between p16 and NCL to hijack NCL-associated machinery of rRNA transcription and pre-rRNA processing to replicate viral gRNA. In addition, the role of p23 in RHDV replication is still unclear. Previous studies have found that, similar to other caliciviruses, RHDV p23 is enriched in the endoplasmic reticulum membrane and plays an important part in inducing intracellular membrane rearrangement (Urakova et al., 2015). Therefore, we believe that p23 interacts with NCL to recruit replication-associated host proteins to the endoplasmic reticulum membrane and assembles these to form membrane-associated RCs.

NCL is an abundant and ubiquitously expressed protein in many growing eukaryotic cells (Jia et al., 2017). NCL is mainly localized within the nucleolus, but it also exists in the nucleoplasm, cytoplasm, and cell surface (Tuteja and Tuteja, 1998; Abdelmohsen and Gorospe, 2012). NCL controls a wide range of fundamental cellular processes, such as ribosome biogenesis, proliferation, and cell cycle regulation, and it also has important roles in the infection process of multiple viruses (Jia et al., 2017). For example, NCL acts as a receptor for human respiratory syncytial virus (Tayyari et al., 2011). NCL also mediates cellular attachment and internalization of enterovirus 71 (Su et al., 2015). A recent study showed that NCL interacted with the capsid protein of dengue virus, suggesting a role in viral morphogenesis (Balinsky et al., 2013). In previous studies, we also found that NCL mediated the internalization of RHDV through interacting with the RHDV capsid protein (Zhu et al., 2018). Of note, NCL also plays an important part in replication of several viruses. For example, NCL interacts with the feline calicivirus (FCV) NS6 (protease) and NS7 (polymerase) proteins, and has a role in virus replication (Cancio-Lonches et al., 2011). Similarly, the interaction between NCL and the UTRs of FCV (Cancio-Lonches et al., 2011) and poliovirus (Waggoner and Sarnow, 1998) stimulates translation of viral proteins. Moreover, NCL binds to a protein of herpes simplex virus type 1 to facilitate the export of US11 from the cell nucleus to the cytoplasm (Sagou et al., 2010). However, the function of NCL in binding to RHDV replicase and recruiting host factors to form RCs had not been revealed until now. Here, we demonstrate for the first time that NCL can specifically bind to RHDV replicase (RdRp) and can act as a link, recruiting host factors and viral proteins, to form RHDV RCs. Our findings enrich the current knowledge about the mechanism of NCL regulation of viral replication and provide new clues for further exploration of the interaction between RHDV and host proteins.

5. Conclusions

In conclusion, we identified the host factors associated with RHDV replicase, for the first time. We found that NCL acted as a link to recruit host factors, viral replicase (RdRp), and nonstructural proteins (p16 and p23), thereby forming a complex and ordered RHDV RC. Elucidation of the molecular mechanism by which NCL regulates viral replicase assembly may lead to new insights into viral RC biogenesis and novel antiviral strategies.

Data availability

All the data generated during the current study are included in the manuscript.

Ethics statement

This article does not contain any studies with human or animal subjects performed by any of the authors.

Author contributions

Jie Zhu: conceptualization, data curation, formal analysis, funding acquisition, writing-original draft. Qiuhong Miao: investigation, validation, writing-review and editing. Hongyuan Guo: investigation, validation. Aoxing Tang: resources, visualization. Dandan Dong: investigation. Jingyu Tang: resources, software. Fang Wang: resources. Guangzhi Tong: conceptualization, methodology, resources. Guangqing Liu: conceptualization, funding acquisition, supervision, project administration, writing-review and editing.

Conflict of interest

The authors declare that they have no conflict of interest.

Acknowledgments

This study was sponsored by Shanghai Sailing Program (20YF1457700), the National Natural Science Foundation of China (32000109 and 31672572), and the China Postdoctoral Science Foundation (2019M660885 and 2021T140718). In addition, we thank LetPub for its linguistic assistance during the preparation of this manuscript.

Appendix A. Supplementary data

Supplementary data to this article can be found online at https://doi.org/10.1016/j.virs.2022.01.004.

References

Abdelmohsen, K., Gorospe, M., 2012. Rna-binding protein nucleolin in disease. RNA Biol. 9, 799–808.
Abrantes, J., Lopes, A.M., Dalton, K.P., Melo, P., Correia, J.J., Ramada, M., Alves, P.C., Parra, F., Esteves, P.J., 2013. New variant of rabbit hemorrhagic disease virus, Portugal, 2012-2013. Emerg. Infect. Dis. 19, 1900–1902.
Alonso, C., Oviedo, J.M., Martín-Alonso, J.M., Díaz, E., Boga, J.A., Parra, F., 1998. Programmed cell death in the pathogenesis of rabbit hemorrhagic disease. Arch. Virol. 143, 321–332.
Aminev, A.G., Amineva, S.P., Palmenberg, A.C., 2003. Encephalomyocarditis viral protein 2a localizes to nucleoli and inhibits cap-dependent mrna translation. Virus Res. 95, 45–57.
Balinsky, C.A., Schmeisser, H., Ganesan, S., Singh, K., Pierson, T.C., Zoon, K.C., 2013. Nucleolin interacts with the dengue virus capsid protein and plays a role in formation of infectious virus particles. J. Virol. 87, 13094–13106.
Becherel, O.J., Gueven, N., Birrell, G.W., Schreiber, V., Suraweera, A., Jakob, B., Taucher-Scholz, G., Lavin, M.F., 2006. Nucleolar localization of aprataxin is dependent on interaction with nucleolin and on active ribosomal DNA transcription. Hum. Mol. Genet. 15, 2239–2249.
Bicknell, K., Brooks, G., Kaiser, P., Chen, H., Dove, B.K., Hiscox, J.A., 2005. Nucleolin is regulated both at the level of transcription and translation. Biochem. Biophys. Res. Commun. 332, 817–822.
Cancio-Lonches, C., Yocupicio-Monroy, M., Sandoval-Jaime, C., Galvan-Mendoza, I., Urena, L., Vashist, S., Goodfellow, I., Salas-Benito, J., Gutierrez-Escolano, A.L., 2011. Nucleolin interacts with the feline calicivirus 3' untranslated region and the protease-polymerase ns6 and ns7 proteins, playing a role in virus replication. J. Virol. 85, 8056–8068.
den Boon, J.A., Ahlquist, P., 2010. Organelle-like membrane compartmentalization of positive-strand rna virus replication factories. Annu. Rev. Microbiol. 64, 241–256.
Dorobantu, C.M., Albulescu, L., Harak, C., Feng, Q., van Kampen, M., Strating, J.R., Gorbalenya, A.E., Lohmann, V., van der Schaar, H.M., van Kuppeveld, F.J., 2015. Modulation of the host lipid landscape to promote rna virus replication: the picornavirus encephalomyocarditis virus converges on the pathway used by hepatitis c virus. PLoS Pathog. 11, e1005185.
Durut, N., Nucleolin, Saez-Vasquez J., 2015. Dual roles in rdna chromatin transcription. Gene 556, 7–12.
Fan, B., Lu, K.Y., Reymond Sutandy, F.X., Chen, Y.W., Konan, K., Zhu, H., Kao, C.C., Chen, C.S., 2014. A human proteome microarray identifies that the heterogeneous nuclear ribonucleoprotein k (hnrnp k) recognizes the 5' terminal sequence of the hepatitis c virus rna. Mol. Cell. Proteomics 13, 84–92.
Hirano, K., Miki, Y., Hirai, Y., Sato, R., Itoh, T., Hayashi, A., Yamanaka, M., Eda, S., Beppu, M., 2005. A multifunctional shuttling protein nucleolin is a macrophage receptor for apoptotic cells. J. Biol. Chem. 280, 39284–39293.
Hsieh, T.Y., Matsumoto, M., Chou, H.C., Schneider, R., Hwang, S.B., Lee, A.S., Lai, M.M., 1998. Hepatitis c virus core protein interacts with heterogeneous nuclear ribonucleoprotein k. J. Biol. Chem. 273, 17651–17659.
Hukowska-Szematowicz, B., 2020. Genetic variability and phylogenetic analysis of lagovirus europaeus strains gi.1 (rhdv) and gi.2 (rhdv2) based on the rna-dependent rna polymerase (rdrp) coding gene. Acta Biochim. Pol. 67, 111–122.
Jia, W., Yao, Z., Zhao, J., Guan, Q., Gao, L., 2017. New perspectives of physiological and pathological functions of nucleolin (ncl). Life Sci. 186, 1–10.
Kovalev, N., Nagy, P.D., 2014. The expanding functions of cellular helicases: the tombusvirus rna replication enhancer co-opts the plant eif4aiii-like atrh2 and the ddx5-like atrh5 dead-box rna helicases to promote viral asymmetric rna replication. PLoS Pathog. 10, e1004051.
Le Gall-Recule, G., Lavazza, A., Marchandeau, S., Bertagnoli, S., Zwingelstein, F., Cavadini, P., Martinelli, N., Lombardi, G., Guerin, J.L., Lemaitre, E., Decors, A., Boucher, S., Le Normand, B., Capucci, L., 2013. Emergence of a new lagovirus related to rabbit haemorrhagic disease virus. Vet. Res. 44, 81.
Le Pendu, J., Abrantes, J., Bertagnoli, S., Guitton, J.S., Le Gall-Recule, G., Lopes, A.M., Marchandeau, S., Alda, F., Almeida, T., Celio, A.P., Barcena, J., Burmakina, G., Blanco, E., Calvete, C., Cavadini, P., Cooke, B., Dalton, K., Delibes Mateos, M., Deptula, W., Eden, J.S., Wang, F., Ferreira, C.C., Ferreira, P., Foronda, P., Goncalves, D., Gavier-Widen, D., Hall, R., Hukowska-Szematowicz, B., Kerr, P., Kovaliski, J., Lavazza, A., Mahar, J., Malogolovkin, A., Marques, R.M., Marques, S., Martin-Alonso, A., Monterroso, P., Moreno, S., Mutze, G., Neimanis, A., Niedzwiedzka-Rystwej, P., Peacock, D., Parra, F., Rocchi, M., Rouco, C., Ruvoen-Clouet, N., Silva, E., Silverio, D., Strive, T., Thompson, G., Tokarz-Deptula, B., Esteves, P., 2017. Proposal for a unified classification system and nomenclature of lagoviruses. J. Gen. Virol. 98, 1658–1666.
Li, T.F., Hosmillo, M., Schwanke, H., Shu, T., Wang, Z., Yin, L., Curry, S., Goodfellow, I.G., Zhou, X., 2018. Human norovirus ns3 has rna helicase and chaperoning activities. J. Virol. 92, e01606–e01617.
Liu, W., Dang, R., Wang, X., 2015. Development of a sybr-based real-time pcr to detect rabbit hemorrhagic disease virus (rhdv) and analyze its tissue distribution in experimentally infected rabbits. Virol. Sin. 30, 228–230.
Lopes, A.M., Rouco, C., Esteves, P.J., Abrantes, J., 2019. Gi.1b/gi.1b/gi.2 recombinant rabbit hemorrhagic disease virus 2 (lagovirus europaeus/gi.2) in Morocco, Africa. Arch. Virol. 164, 279–283.
Maggi Jr., L.B., Kuchenruether, M., Dadey, D.Y., Schwope, R.M., Grisendi, S., Townsend, R.R., Pandolfi, P.P., Weber, J.D., 2008. Nucleophosmin serves as a rate-limiting nuclear export chaperone for the mammalian ribosome. Mol. Cell Biol. 28, 7050–7065.
Mahar, J.E., Read, A.J., Gu, X., Urakova, N., Mourant, R., Piper, M., Haboury, S., Holmes, E.C., Strive, T., Hall, R.N., 2018. Detection and circulation of a novel rabbit hemorrhagic disease virus in Australia. Emerg. Infect. Dis. 24, 22–31.
Meyers, G., 2003. Translation of the minor capsid protein of a calicivirus is initiated by a novel termination-dependent reinitiation mechanism. J. Biol. Chem. 278, 34051–34060.
Meyers, G., Wirblich, C., Thiel, H.J., 1991a. Genomic and subgenomic rnas of rabbit hemorrhagic disease virus are both protein-linked and packaged into particles. Virology 184, 677–686.
Meyers, G., Wirblich, C., Thiel, H.J., 1991b. Rabbit hemorrhagic disease virus–molecular cloning and nucleotide sequencing of a calicivirus genome. Virology 184, 664–676.
Mikami, D., Park, J.H., Kimura, T., Ochiai, K., Itakura, C., 1999. Hepatic lesions in young rabbits experimentally infected with rabbit haemorrhagic disease virus. Res. Vet. Sci. 66, 237–242.
Mongelard, F., Nucleolin, Bouvet P., 2007. A multifaceted protein. Trends Cell Biol. 17, 80–86.
Morales, M., Barcena, J., Ramirez, M.A., Boga, J.A., Parra, F., Torres, J.M., 2004. Synthesis in vitro of rabbit hemorrhagic disease virus subgenomic rna by internal initiation on (-)sense genomic rna: mapping of a subgenomic promoter. J. Biol. Chem. 279, 17013–17018.
Nüesch, J.P.F., Rommelaere, J., 2006. Ns1 interaction with ckiiα: novel protein complex mediating parvovirus-induced cytotoxicity. J. Virol. 80, 4729–4739.
Nagy, P.D., Pogany, J., 2011. The dependence of viral rna replication on co-opted host factors. Nat. Rev. Microbiol. 10, 137–149.
Neimanis, A., Larsson Pettersson, U., Huang, N., Gavier-Widén, D., Strive, T., 2018. Elucidation of the pathology and tissue distribution of lagovirus europaeus gi.2/rhdv2 (rabbit haemorrhagic disease virus 2) in young and adult rabbits (oryctolagus cuniculus). Vet. Res. 49, 46.
Oliveira, L.M., Blawid, R., Orilio, A.F., Andrade, B.Y.G., Souza, A.C.A., Nagata, T., 2018. Development of an infectious clone and replicon system of norovirus gii.4. J. Virol. Methods 258, 49–53.
Robledo, S., Idol, R.A., Crimmins, D.L., Ladenson, J.H., Mason, P.J., Bessler, M., 2008. The role of human ribosomal proteins in the maturation of rrna and ribosome production. RNA 14, 1918–1929.
Rouco, C., Abrantes, J., Serronha, A., Lopes, A.M., Maio, E., Magalhaes, M.J., Blanco, E., Barcena, J., Esteves, P.J., Santos, N., Alves, P.C., Monterroso, P., 2018. Epidemiology of rhdv2 (lagovirus europaeus/gi.2) in free-living wild european rabbits in Portugal. Transbound Emerg. Dis. 65, e373–e382.
Sagou, K., Uema, M., Kawaguchi, Y., 2010. Nucleolin is required for efficient nuclear egress of herpes simplex virus type 1 nucleocapsids. J. Virol. 84, 2110–2121.
Saxena, V., Lai, C.K., Chao, T.C., Jeng, K.S., Lai, M.M., 2012. Annexin a2 is involved in the formation of hepatitis c virus replication complex on the lipid raft. J. Virol. 86, 4139–4150.
Su, P.Y., Wang, Y.F., Huang, S.W., Lo, Y.C., Wang, Y.H., Wu, S.R., Shieh, D.B., Chen, S.H., Wang, J.R., Lai, M.D., Chang, C.F., 2015. Cell surface nucleolin facilitates enterovirus 71 binding and infection. J. Virol. 89, 4527–4538.
Subba-Reddy, C.V., Yunus, M.A., Goodfellow, I.G., Kao, C.C., 2012. Norovirus rna synthesis is modulated by an interaction between the viral rna-dependent rna polymerase and the major capsid protein, vp1. J. Virol. 86, 10138–10149.
Tayyari, F., Marchant, D., Moraes, T.J., Duan, W., Mastrangelo, P., Hegele, R.G., 2011. Identification of nucleolin as a cellular receptor for human respiratory syncytial virus. Nat. Med. 17, 1132–1135.
Thackray, L.B., Duan, E., Lazear, H.M., Kambal, A., Schreiber, R.D., Diamond, M.S., Virgin, H.W., 2012. Critical role for interferon regulatory factor 3 (irf-3) and irf-7 in type i interferon-mediated control of murine norovirus replication. J. Virol. 86, 13515–13523.
Thorne, L.G., Goodfellow, I.G., 2014. Norovirus gene expression and replication. J. Gen. Virol. 95, 278–291.
Tuteja, R., Tuteja, N., 1998. Nucleolin: a multifunctional major nucleolar phosphoprotein. Crit. Rev. Biochem. Mol. Biol. 33, 407–436.
Urakova, N., Strive, T., Frese, M., 2017a. Rna-dependent rna polymerases of both virulent and benign rabbit caliciviruses induce striking rearrangement of golgi membranes. PLoS One 12, e0169913.
Urakova, N., Warden, A.C., White, P.A., Strive, T., Frese, M., 2017b. A motif in the f homomorph of rabbit haemorrhagic disease virus polymerase is important for the

subcellular localisation of the protein and its ability to induce redistribution of golgi membranes. Viruses 9, 202.
Urakova, N., Frese, M., Hall, R.N., Liu, J., Matthaei, M., Strive, T., 2015. Expression and partial characterisation of rabbit haemorrhagic disease virus non-structural proteins. Virology 484, 69–79.
Waggoner, S., Sarnow, P., 1998. Viral ribonucleoprotein complex formation and nucleolar-cytoplasmic relocalization of nucleolin in poliovirus-infected cells. J. Virol. 72, 6699–6709.
Wang, B., Zhe, M., Chen, Z., Li, C., Meng, C., Zhang, M., Liu, G., 2013. Construction and applications of rabbit hemorrhagic disease virus replicon. PLoS One 8, e60316.
Wirblich, C., Sibilia, M., Boniotti, M.B., Rossi, C., Thiel, H.J., Meyers, G., 1995. 3c-like protease of rabbit hemorrhagic disease virus: Identification of cleavage sites in the orf1 polyprotein and analysis of cleavage specificity. J. Virol. 69, 7159–7168.
Yi, Z., Fang, C., Zou, J., Xu, J., Song, W., Du, X., Pan, T., Lu, H., Yuan, Z., 2016. Affinity purification of the hepatitis c virus replicase identifies valosin-containing protein, a member of the atpases associated with diverse cellular activities family, as an active virus replication modulator. J. Virol. 90, 9953–9966.
Zhang, C., He, L., Kang, K., Chen, H., Xu, L., Zhang, Y., 2014. Screening of cellular proteins that interact with the classical swine fever virus non-structural protein 5a by yeast two-hybrid analysis. J. Biosci. 39, 63–74.
Zhu, J., Miao, Q., Tan, Y., Guo, H., Li, C., Chen, Z., Liu, G., 2016. Extensive characterization of a lentiviral-derived stable cell line expressing rabbit hemorrhagic disease virus vpg protein. J. Virol. Methods 237, 86–91.
Zhu, J., Wang, B., Miao, Q., Tan, Y., Li, C., Chen, Z., Guo, H., Liu, G., 2015. Viral genome-linked protein (vpg) is essential for translation initiation of rabbit hemorrhagic disease virus (rhdv). PLoS One 10, e0143467.
Zhu, J., Miao, Q., Tan, Y., Guo, H., Liu, T., Wang, B., Chen, Z., Li, C., Liu, G., 2017. Inclusion of an arg-gly-asp receptor-recognition motif into the capsid protein of rabbit hemorrhagic disease virus enables culture of the virus in vitro. J. Biol. Chem. 292, 8605–8615.
Zhu, J., Miao, Q., Tang, J., Wang, X., Dong, D., Liu, T., Qi, R., Yang, Z., Liu, G., 2018. Nucleolin mediates the internalization of rabbit hemorrhagic disease virus through clathrin-dependent endocytosis. PLoS Pathog. 14, e1007383.